

Influence of doping methods and Nd^{3+} concentration on the formation of dipole and activator centers in $\text{PbMoO}_4:\text{Nd}^{3+}$ and $\text{PbWO}_4:\text{Nd}^{3+}$ crystals

Y.N.Gorobets, B.P.Nazarenko, A.N.Shekhovtsov

Institute for Single Crystals, STC "Institute for Single Crystals" National Academy of Sciences of Ukraine,
60 Lenin Ave., 61001 Kharkiv, Ukraine

Received April 17, 2013

Equivalent circuits were used to study peculiarities of polarization processes in $\text{PbMoO}_4:\text{Nd}^{3+}$ and $\text{PbWO}_4:\text{Nd}^{3+}$ crystals depending on a doping method. The method of doping was found to influence the formation of dipoles defining the polarization processes in these crystals. On the base of the obtained data the models of activator centers in $\text{PbMoO}_4:\text{Nd}^{3+}$ and $\text{PbWO}_4:\text{Nd}^{3+}$ crystals are proposed.

С помощью эквивалентных схем замещения изучены особенности поляризационных процессов в кристаллах $\text{PbMoO}_4:\text{Nd}^{3+}$, $\text{PbWO}_4:\text{Nd}^{3+}$, активированных различными способами. Установлено влияние способа введения активатора на формирование диполей, определяющих процессы поляризации в этих кристаллах. На основании полученных данных предложены модели активаторных центров в кристаллах $\text{PbMoO}_4:\text{Nd}^{3+}$ и $\text{PbWO}_4:\text{Nd}^{3+}$.

1. Introduction

One of significant parameters of the crystals simultaneously used as active laser medium and SRS converter is the damage threshold. This is bound up with considerable rise of the efficiency of SRS transformation depending on the pumping power [1]. The study of $\text{PbMoO}_4:\text{Nd}^{3+}$ (PMO) crystal damage threshold depending on the doping method allowed to establish the dependence of the damage threshold of these crystals on the doping method and the Nd^{3+} concentration in the crystals [2]. The change of the damage threshold may be caused by the appearance of activator centers in the crystal. These centers can affect the formation of electron avalanche at absorption of laser radiation and serve as centers of localization or delocalization of electrons. Thus, the activator centers can raise

or reduce the damage threshold of the crystals. The change of the activator center structure depends on the concentration of the dopant in the crystals and the method of doping. Structural inhomogeneties strongly influence the dielectric properties of the crystals, in particular, the activation energy of relaxation processes. Therefore, the study is devoted to the investigation of $\text{PMO}:\text{Nd}^{3+}$ and $\text{PbWO}_4:\text{Nd}^{3+}$ (PWO) crystals by means of dielectric relaxation spectroscopy depending on the Nd^{3+} concentration and doping method.

2. Experimental

Nd^{3+} -doped, PMO and PWO single crystals were grown in air from Pt-crucibles by the Czochralski method using the "Analog" automatic set-up equipped with a weight control system. To dope PMO crystals Nd_2O_3 (sample #1), as well as previously

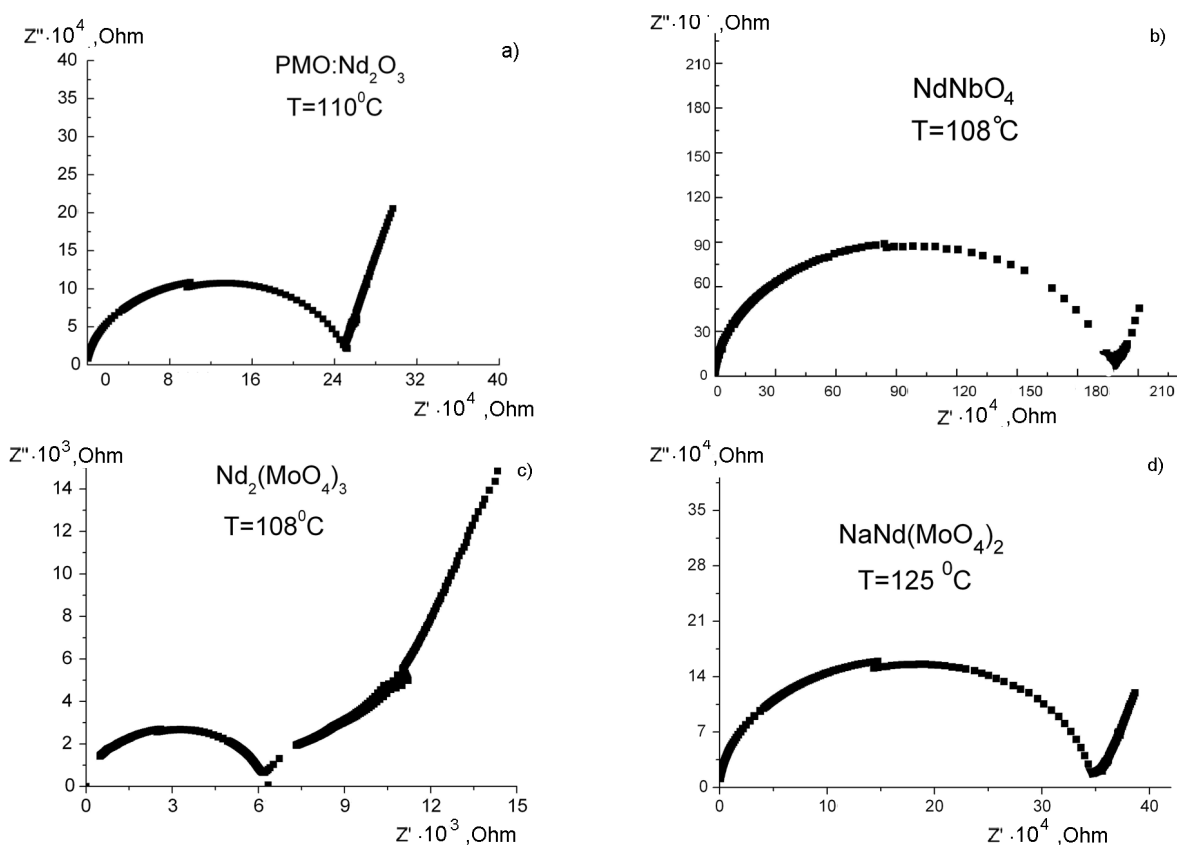


Fig. 1. Cole-Cole plots of complex impedance for $\text{PbMoO}_4:\text{Nd}^{3+}$ crystals: a — $\text{PbMoO}_4:\text{Nd}_2\text{O}_3$, b — $\text{PbMoO}_4:\text{NdNbO}_4$, c — $\text{PbMoO}_4:\text{Nd}_2(\text{MoO}_4)_3$, d — $\text{PbMoO}_4:\text{NaNd}(\text{MoO}_4)_2$.

synthesized $\text{Nd}_2(\text{MoO}_4)_3$ (sample #2), $\text{NaNd}(\text{MoO}_4)_2$ (sample #3) and NdNbO_4 (sample #4) compounds were used. To dope PWO crystals $\text{Nd}_2(\text{WO}_4)_3$ was used only. The growth parameters were the same for all the crystals.

E7-20 impedance meter was used for impedance analysis. Au contacts were sputtered on opposing planes. Dielectric measurements were carried out at various temperatures ranging from 300–600 K and with various frequencies ranging from 25 Hz–1 MHz by use the parallel plate capacitor method. Every temperature step was stabilized for 30 min.

3. Results and discussion

The dielectric and optical properties of $\text{PbMoO}_4:\text{Nd}^{3+}$ crystals doped with Nd^{3+} using different compounds, as well as the samples of the crystals with different Nd^{3+} concentrations were investigated in [3, 4]. This study allowed to establish essential differences between the activation energies of relaxation processes in these crystals. Depending on a doping method of crystal one or few activation energies were observed.

The magnitudes of activation energies were different. The curve of luminescence decay of $\text{Nd}^{3+} \ ^4F_{3/2} \rightarrow \ ^4I_{11/2}$ transition was approximated by one or sum of two exponents. The constants of decay time were different, too. Such distinctions may be caused by different surrounding of Nd^{3+} ions in the crystal lattice [4].

In the mentioned papers we determined the values of activation energy for the relaxation processes observed in the crystals, from the analysis of the graphs of the dependences $\ln(F_{max})$ on $1/T$, where F_{max} are the maxima of the curves of dielectric loss angle tangent, T , the temperature in Kelvin degrees. In the general case the relaxation process can be characterized by the presence of one or several dipoles and have the form of the superposition of several relaxation processes with an averaged activation energy. Separation of individual constituents of the relaxation processes may be useful at determination of the dipoles which form the said process.

To get more information about the polarization processes in the crystals, the obtained data were treated by simulating these processes by means of equivalent cur-

circuits (EC). For this purpose, the experimental frequency-temperature dependences of capacitance $C = f(F, T)$ and conductivity $G = f(F, T)$ of the samples were used to calculate the complex impedance $Z = Z' + Z''$ (Fig. 1). Then, the EC of the sample was calculated by the method of numerical simulation (Fig. 2).

Using the method of successive approximations and changing the values of the EC elements, we achieved the coincidence for the simulated and experimental data: $Z'' = f(Z')$. This allowed to determine the values of the elements for the EC of the samples doped by different methods (Table 1). The X-ray diffractometry data are presented in Table 2 [6]. As seen from this Table, in all the cases Nd^{3+} ions occupy the crystallographic positions of Pb^{2+} . The samples #1, #2 and #3 are found to contain vacancies in the Mo^{6+} sublattice (— are molybdenum vacancies). In the sample #4 vacancies in the sublattice Mo^{6+} are not. It is established that Na^+ ions (sample #3) occupy the crystallographic positions of Pb^{2+} .

As seen from Fig. 1a–d, the Cole-Cole plots obtained for different crystals essentially differ. According to [3, 4] the samples #1 and #2 are characterized by different number activation energies of the relaxation processes, as well as by different number of the luminescence decay times. Essential distinctions are also observed in the Cole-Cole plots calculated for these Samples (Fig. 1a, c) and, consequently, in the EC and the values of their elements (Table 1). In particular,

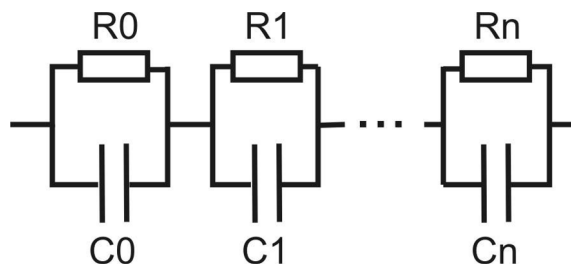


Fig. 2. Equivalent RC circuits used for the simulation of the relaxation processes.

the EC for Sample #1 has 3 circuits, whereas that for Sample 2 contains 4 circuits. Thereat, the values of EC parameters essentially differ. This can testify to considerable distinctions in the dipoles for these samples. On the other hand, in accordance with the data contained in Table 2, there are no essential difference in the real compositions of these samples. Both crystals have approximately the same Nd^{3+} concentration. According to the X-ray structure data (Table 2), the Nd^{3+} ions occupy the same crystallographic positions — those of Pb^{2+} . Both samples contain molybdenum vacancies and do not have vacancies in the oxygen sublattice.

Thus, essential distinctions in the dipoles observed in these samples may be explained by different location of the molybdenum and Nd^{3+} vacancies with comparatively to each other in the crystal lattice. Proceeding from the structural formulae determined by means of X-ray diffractometry, the most

Table 1. RC circuits and their values for $\text{PbMoO}_4:\text{Nd}^{3+}$ crystals

	Sample #1; 0.75 wt. %		Sample #2; 0.8 wt. %		Sample #3; 0.8 wt. %		Sample #4; 0.8 wt. %	
	C, pF	R, Ohm	C, pF	R, Ohm	C, pF	R, Ohm	C, pF	R, Ohm
1	60700	$3 \cdot 10^5$	3	$1.95 \cdot 10^6$	100	6200	5	$3.4 \cdot 10^5$
2	60700	$2.55 \cdot 10^6$	$7 \cdot 10^5$	$1 \cdot 10^6$	$4 \cdot 10^4$	2500	$1.7 \cdot 10^4$	$2 \cdot 10^4$
3	8	$2.55 \cdot 10^5$	—	—	$1.5 \cdot 10^5$	3500	$5 \cdot 10^4$	$4 \cdot 10^5$
4	—	—	—	—	$2.1 \cdot 10^5$	$1 \cdot 10^5$	—	—
E_a , eV	0.45		0.46		0.24, 0.27, 0.37		0.32, 0.51	

Table 2. The composition of $\text{PbMoO}_4:\text{Nd}^{3+}$ crystals

#	Crystal	Structure formula
1	$\text{PbMoO}_4:\text{Nd}_2\text{O}_3$	$(\text{Pb}^{2+}_{0.970(2)}\text{Nd}^{3+}_{0.030})(\text{Mo}^{6+}_{0.995(2)}\text{—}_{0.005})\text{O}_4$
2	$\text{PbMoO}_4:\text{Nd}_2(\text{MoO}_4)_3$	$(\text{Pb}^{2+}_{0.980(2)}\text{Nd}^{3+}_{0.020})(\text{Mo}^{6+}_{0.997(2)}\text{—}_{0.003})\text{O}_4$
3	$\text{PbMoO}_4:\text{NaNd}(\text{MoO}_4)_2$	$(\text{Pb}^{2+}_{0.954}\text{Nd}^{3+}_{0.035}\text{Na}^+_{0.011})(\text{Mo}^{6+}_{0.996(2)}\text{—}_{0.004})\text{O}_4$
4	$\text{PbMoO}_4:\text{NdNbO}_4$	$(\text{Pb}^{2+}_{0.975(2)}\text{Nd}^{3+}_{0.025})(\text{Mo}^{6+}_{0.975}\text{Nb}^{5+}_{0.025})\text{O}_4$

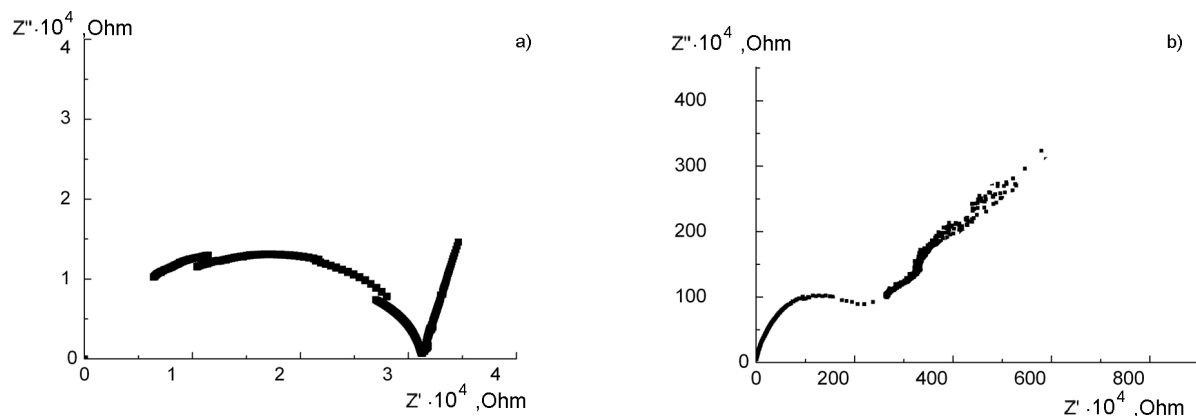


Fig. 3. Cole-Cole plots of complex impedance for $\text{PbWO}_4:\text{Nd}^{3+}$: a — 1.5 wt.%, b — 1.7 wt.%.

probable way of charge compensation for Sample #1 and Sample #2 is $6(\text{Nd}_{\text{Pb}}^{3+})^{\bullet} + (\text{V}_{\text{Mo}}^{6+})^{\prime\prime\prime\prime}$ [3]. Thereat, in the former case, the neodymium ions and molybdenum vacancies will be uniformly distributed in the bulk of the sample, whereas in the latter case they will be located close to each other. Insignificant distinction in the activation energies in Sample #2 may be caused by different special location of Mo^{6+} vacancies and Nd^{3+} ions in the crystal lattice. In the case when the crystals are doped with $\text{NaNd}(\text{MoO}_4)_2$ (3), the Cole-Cole plots is simulated by means of the EC including 3 circuits. The resistances in the circuits are higher in comparison with those in the samples doped with $\text{Nd}_2(\text{MoO}_4)_3$, but lower than the ones in the rest of the samples.

Since in this case the ions of neodymium and sodium are located in the lead sublattice, the charge compensation is most likely realized according either to the scheme $6(\text{Nd}_{\text{Pb}}^{3+})^{\bullet} + (\text{V}_{\text{Mo}})^{\prime\prime\prime\prime}$ or to the scheme $(\text{Nd}_{\text{Pb}}^{3+})^{\bullet} + (\text{Na}_{\text{Pb}})^{\prime}$, that gives rise to the appearance of an additional contour in the EC in comparison to the EC calculated for samples #1 (Nd_2O_3).

The structural formula of the sample #4 distinguishes from the rest formulae by the absence of molybdenum vacancies. This confirms the assumption that in this case the charge compensation is realized according to the scheme $(\text{Nd}_{\text{Pb}}^{3+})^{\bullet} + (\text{Nb}_{\text{Mo}}^{5+})^{\prime}$. The EC of the sample is characterized by the presence of only two circuits with high resistances. Thereat, the temperature at which the Cole-Cole plots suitable for the analysis was obtained, considerably exceeded the corresponding temperatures for the rest of the samples. This speaks for an essential role of the molybdenum vacancies in the formation of the observed dipoles.

There were obtained the $\text{PbWO}_4:\text{Nd}^{3+}$ crystals containing Nd^{3+} 1.5 (sample #5) and 1.7 (sample #6) wt. % of Nd^{3+} . The Cole-Cole diagrams are presented in Fig. 3. As show the data contained in Table 3, the rise of Nd^{3+} concentration in the crystal $\text{PbWO}_4:\text{Nd}^{3+}$ leads to changes of its dielectric properties. Unfortunately, we could not manage to determine the parameters of the circuits with high-resistance constituents. Such circuits are denoted as "*". However, as seen from the Fig. 3, the circuits with low-resistance constituents undergo essen-

Table 3. RC circuits and their values for $\text{PbWO}_4:\text{Nd}^{3+}$ crystals

#	1.5 wt.% Nd^{3+}		1.7 wt.% Nd^{3+}	
	C, pF	R, Ohm	C, pF	R, Ohm
1	13	15×10^3	20	2.2×10^6
2	40	16.4×10^3	600	2.3×10^6
3	450×10^3	55×10^6	3200	4.3×10^6
4	*	*	15000	1×10^6
5	—	—	*	*
E_a , eV	0.6		0.48	

tial changes. The resistance in the circuits and their number considerably increase with the concentration of neodymium. This unambiguously points to essential transformation of the dipoles in the crystal.

It is known that the most probable way of the charge compensation in $\text{PbWO}_4:\text{Nd}^{3+}$ crystal is $2(\text{Nd}_{\text{Pb}}^{3+})^\bullet + (\text{V}_{\text{Pb}})''$ [6]. The rise of Nd^{3+} concentration is accompanied with the transformation of the activator center into $(\text{Nd}_{\text{Pb}}^{3+})^\bullet + (\text{Nd}_{\text{W}}^{3+})''' - (\text{V}_{\text{O}})''$ [6]. This may be the cause of the changes in the dielectric and optical properties of $\text{PbWO}_4:\text{Nd}^{3+}$ crystals at the increase of the concentration of neodymium.

4. Conclusions

According to the simulation of polarization processes results by means of equivalent circuits it was shown, that depending on a concentration and doping method of crystal the different types of dipoles are formed. In particular, the use of Nd_2O_3 and $\text{Nd}_2(\text{MoO}_4)_3$ compounds leads to the same composition crystals, but with essentially different dipoles observed in these crystals. It is

found that the vacancies of Mo influence the relaxation processes in the crystals.

The use of the co-activators Na and Nb leads to the change of activation energies in comparison to $\text{PMO}:\text{Nd}_2\text{O}_3$. Similar changes are also observed for $\text{PWO}:\text{Nd}^{3+}$ crystals when the concentration of Nd in the crystals rises from 1.5 to 1.7 wt. %. Based on the results of [3–5] and the data obtained in the present study, the models of activator centers formed in $\text{PbMoO}_4:\text{Nd}^{3+}$ and $\text{PbWO}_4:\text{Nd}^{3+}$ crystals are proposed.

References

1. T.T.Basiev, *Uspekhi Fiz.*, **169**, 1149 (1999).
2. T.T.Basiev, V.N.Baumer et al., *Crystallography Rep.*, **54**, 741 (2009).
3. Y.N.Gorobets, M.B.Kosmyrna, B.P.Nazarenko et al., *J.Cryst. Growth*, **318**, 687 (2010).
4. Yu.N.Gorobets, M.B.Kosmyrna, B.P.Nazarenko et al., *Crystallography Rep.*, **57**, 962 (2012).
5. Yu.N.Gorobets, M.B.Kosmyrna, B.P.Nazarenko et al., in: Abstr. of International Conference RK SNG, Kharkiv, Ukraine (2012), P92(A2).
6. Weifeng Li, Hongwei Huang, Xiqi, *Phys. Stat. Sol.*, **202**, 2531 (2005).

Вплив способів активації і концентрації Nd^{3+} на формування диполів і активаторних центрів у кристалах $\text{PbMoO}_4:\text{Nd}^{3+}$ і $\text{PbWO}_4:\text{Nd}^{3+}$

Ю.М.Горобець, О.М.Шеховцов, Б.П.Назаренко

За допомогою еквівалентних схем заміщення вивчено особливості поляризаційних процесів у кристалах $\text{PbMoO}_4:\text{Nd}^{3+}$, $\text{PbWO}_4:\text{Nd}^{3+}$ активованих різними способами. Установлено вплив способу введення активатора на формування диполів, які визначають процеси поляризації у цих кристалах. На підставі отриманих даних запропоновано моделі активаторних центрів у кристалах $\text{PbMoO}_4:\text{Nd}^{3+}$ і $\text{PbWO}_4:\text{Nd}^{3+}$.